Flavonoid Derivatives as Adenosine Receptor Antagonists: A Comparison of the Hypothetical Receptor Binding Site Based on a Comparative Molecular Field Analysis Model

Stefano Moro, A. Michiel van Rhee, Lawrence H. Sanders, and Kenneth A. Jacobson*

Molecular Recognition Section, Laboratory of Bioorganic Chemistry, National Institute of Diabetes, Digestive and Kidney Diseases, National Institutes of Health, Bethesda, Maryland 20892

Flavonoid derivatives have been optimized as relatively rigid antagonists of adenosine receptors with particular selectivity for the A_3 receptor subtype. A quantitative study of the structure-activity relationships for binding of flavonoids to adenosine A_1, A_{2A}, and A_3 receptors has been conducted using comparative molecular field analysis (CoMFA). Correlation coefficients (cross-validated r^2) of 0.605, 0.595, and 0.583 were obtained for the three subtypes, respectively. All three CoMFA models have the same steric and electrostatic contributions, implying similar requirements inside the binding cavity. Similarities were seen in the topology of steric and electrostatic regions with the A_1 and A_3 receptors, but not the A_{2A}. Substitutions on the phenyl ring at the C-2 position of the chromone moiety may be considered important for binding affinity at all adenosine receptors. In the A_3 model a region of favorable bulk interaction is located around the 2′-position of the phenyl ring. The presence of a C-6 substituent in the chromone moiety is well tolerated and increases the A_1/A_3 selectivity. The CoMFA coefficient contour plots provide a self-consistent picture of the main chemical features responsible for the pK_i variations and also result in predictions which agree with experimental values.

Introduction

A wide variety of non-purine ligands that bind selectively to adenosine receptors have been described.[1,2] The availability of selective ligands has facilitated studies of the physiological roles of particular subtypes of adenosine receptors. A_3 adenosine receptors are associated with cerebroprotective[3] and cardioprotective[4] effects of adenosine agonists and effects on the immune and inflammatory systems.[5] Unlike A_1 and A_2 subtypes, for A_3 receptor xanthine derivatives have not proven to be suitable leads for the development of antagonists for this subtype. We have introduced A_3 receptor-selective antagonists belonging to three distinct, non-purine chemical classes: flavonoids,[6,7] 1,4-dihydropyridines,[8,9] and [1,2,4]triazolo[1,5-*c*]quinazolines.[10] Recently we have synthesized antagonists in the dihydropyridine class with A_3 receptor selectivities of >30000-fold.[9] Other A_3 receptor antagonists belonging to triazolo-[5,1-*a*][2,7]naphthyridine and thiazolo[3,2]pyrimidine classes[11] have been identified through broad screening at Merck. A_3 receptor-selective antagonists have been suggested to have antiasthmatic[12] and possibly cerebroprotective[13] properties.

A broad screening of phytochemicals in competitive binding versus the high-affinity agonist [^{125}I]AB-MECA (N^6-(4-amino-3-iodobenzyl)adenosine 5′-*N*-methyluron-amide) has demonstrated micromolar affinity of assays certain naturally occurring flavonoids at cloned human brain A_3-adenosine receptors.[6] The considerable affinity of flavones at adenosine receptors may explain some of the previously observed vascular and other biological effects of these compounds. Starting from structure−activity relationships, chemical optimization of this class led to 3,6-dichloro-2′-(isopropyloxy)-4′-methylflavone[7] (MRS 1067; K_i = 0.56 μM), which is both relatively potent and highly selective (200-fold) for human A_3 vs human A_1 receptors. This derivative effectively antagonized the effects of an agonist in the inhibition of adenylyl cyclase in Chinese hamster ovary (CHO) cells expressing either cloned rat or human A_3 receptors.[7,14] MRS 1067 antagonized the effects of the A_3 receptor-selective agonist Cl-IB-MECA to induce a rise in intracellular [Ca^{2+}] in RBL-2H3 rat mast cells.[15]
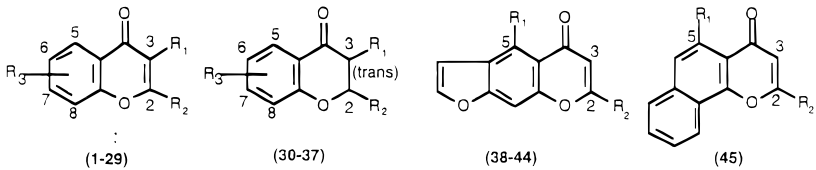
A dramatic species dependence of A_3 receptor affinity has been observed for most classes of antagonists,[9,16,17] and the affinity at the human subtype is usually considerably higher than in the rat. Although nanomolar affinity has not yet been achieved for flavonoids binding at A_3 receptors, the unique characteristic of this class of antagonists is that the ratio of affinities at human vs rat A_3 receptors is only 1 order of magnitude.[6]

Moreover flavonoids are known to bind to a wide range of enzymes,[18−21] in addition to adenosine receptors, and these actions may interfere with their use as pharmacological probes at A_3 receptors. In particular, MRS 1067 was found to bind to rat liver cytochrome P450s.[21]

Thus, we have embarked on a quantitative study of the structure−activity relationships of flavonoids binding to adenosine A_1, A_{2A}, and A_3 receptors, using comparative molecular field analysis (CoMFA) in an effort to develop novel A_3 adenosine antagonists. The

* Address correspondence to: Dr. Kenneth A. Jacobson, Chief, Molecular Recognition Section, NIH/NIDDK/LBC, Bldg. 8A, Rm B1A-19, Bethesda, MD 20892-0810. Tel: (301) 496-9024. FAX: (301) 480-8422. E-mail: kajacobs@helix.nih.gov.

Table 1. Observed and Calculated Receptor-Binding Affinity Values of the Compounds Forming A_1, A_{2A}, and A_3 Training Sets

| | | | | pK_i $(\mu M)^a$ | | | | | |
| | | | | rA$_1$ | | rA$_{2A}$ | | hA$_3$ | |
compound	R$_1$	R$_2$	R$_3$	obsd	calcd^b	obsd	calcd^b	obsd	calcd^b
1 (galangin)	OH	Ph	5,7-(OH)$_2$	ts	ts	ts	ts	−0.23	−0.26
2 (MRS928)	OMe	Ph	5,7-(OMe)$_2$	0.29	0.31	−0.81	−0.75	−0.08	−0.08
3 (MRS1041)	OEt	Ph	5,7-(OEt)$_2$	0.22	0.33	−0.52	−0.54	0.44	0.37
4 (MRS1093)	OEt	Ph	5-OH−7-OEt	−0.28	−0.37	−1.80	−1.78	0.13	0.16
5 (MRS1042)	OPr	Ph	5,7-(OPr)$_2$	−0.04	−0.04	−0.51	−0.54	0.50	0.44
6	CH$_2$CH=C(CH$_3$)$_2$	2′,4′-(OH)$_2$Ph	5-OH-6-CH=CHCH(CH$_3$)$_2$-7-(OMe)$_2$	−0.96	−0.99	na		−0.66	−0.67
7 (MRS923)	OMe	2′,4′-(OMe)$_2$Ph	5,7-(OMe)$_2$	−1.44	−1.47	−1.67	−1.57	−0.42	−0.50
8 (MRS1063)	OEt	2′,4′-(OEt)$_2$Ph	5-OH−7-OEt	na		na		−0.68	−0.70
9 (MRS1086)	OEt	2′,4′-(OEt)$_2$Ph	5,7-(OEt)$_2$	−1.51	−1.53	−1.42	−1.46	−0.86	−0.78
10	OH	2′,4′,6′-(OMe)$_3$Ph	H	−0.86	−0.76	na		−1.70	−1.73
11 (MRS1132)	Cl	Ph	H	ts	ts	−1.40	−1.39	−1.06	−0.98
12 (MRS1088)	Cl	Ph	6-Cl	na		−1.74	−1.65	ts	ts
13 (MRS1067)	Cl	2′-*i*-Pr-4′-MePh	6-Cl	na		na		0.25	0.32
14	H	Ph	5-OH	−0.34	−0.38	na		na	
15	H	Ph	7-OH	−0.48	−0.41	−0.43	−0.43	na	
16	H	3′,4′-(MeO)$_2$Ph	7-OH	−1.27	−1.30	−1.54	−1.59	na	
17 (apigenin)	H	4′-OHPh	5,7-(OH)$_2$	−0.48	−0.47	−0.88	−0.92	na	
18	H	4′-OMePh	5-OH−7-Me	−0.53	−0.49	−1.45	−1.40	−1.70	−1.69
19	H	4′-MeOPh	5,6,7-(OMe)$_3$	−0.11	−0.08	na		−0.65	−0.69
20 (hispidulin)	H	4′-OHPh	5,7-(OH)$_2$-6−MeO	−0.21	−0.23	−0.88	−0.88	na	
21 (cirsimaritin)	H	4′-OHPh	5-OH−6,7-(MeO)$_2$	−0.08	−0.02	−0.48	−0.49	−0.50	−0.35
22	OMe	Ph	5,7-(MeO)$_2$	0.29	0.23	−0.81	−0.73	−0.09	0.01
23	OAc	Ph	5,7-(AcO)$_2$	−1.06	−1.03	na		−1.24	−1.27
24	OMe	4′-OMePh	5,7-(MeO)$_2$	−0.03	−0.02	na		−0.53	0.55
25 (rhamnetin)	OH	3′,4′-(OH)$_2$Ph	7-OMe	na		na		−0.14	−0.13
26 (quercitin)	OH	3′,4′-(OH)$_2$Ph	5,7-(OH)$_2$	−0.39	−0.33	−0.84	−0.86	na	
27 (pentamethylmorin)	OMe	2′,4′-(MeO)$_2$Ph	5,7-(MeO)$_2$	−1.44	−1.34	−1.67	−1.75	−0.42	−0.47
28 (hexamethylmyricetin)	OMe	3′,4′,5′-(MeO)$_3$Ph	5,7-(MeO)$_2$	na		na		−0.82	−0.73
29 (flavone)	H	Ph	H	−0.52	−0.52	−0.54	−0.48	−1.23	−1.18
30 (flavanone)	H	Ph	H	ts	ts	na		−1.21	−1.16
31	H	2′-OHPh	H	−0.42	−0.57	−1.25	−1.25	−0.78	−0.89
32	H	4′-OHPh	H	−1.06	−1.15	na		−1.36	−1.40
33 (sakuranetin)	H	4′-OHPh	5-OH−7-OMe	−0.91	−0.89	−1.55	−1.63	−0.53	−0.63
34	OH	2′-OHPh	H	−1.96	−1.90	na		na	
35 (MRS1061)	OH	CH=CHPh	6-OMe	na		na		−1.32	−1.32
36 (MRS1062)	OH	CH=CPh	6-OMe	−1.70	−1.67	na		−0.91	−0.89
37 (dihydroquercitin)	OH	3′,4′-(OH)$_2$Ph	5,7-(OH)$_2$	na		na		−1.53	−1.55
38 (visnagin)	OCH$_3$	CH$_3$		na		−1.63	−1.66	−1.78	−1.77
39	OCH$_3$	CHO		na		na		−1.95	−1.95
40 (MRS1065)	OCH$_3$	CH=CHPh		−1.51	−1.52	−1.06	−1.28	−0.92	−0.94
41 (MRS1066)	OC$_2$H$_5$	CH=CHPh		−1.55	−1.59	−1.53	−1.45	−0.06	−0.12
42 (MRS1084)	O(CH$_2$)$_2$CH$_3$	CH=CHPh		−1.60	−1.61	−1.69	−1.55	−0.60	−0.71
43 (MRS1071)	OC$_2$H$_5$	CH=CHCH=CHPh		na		−2.22	−2.19	−1.66	−1.58
44 (MRS1078)	OCH$_3$	CH=NPh		na		na		−0.96	−0.96
45 (α-naphthoflavone)	H	Ph		0.10	0.14	−0.12	−0.15	na	

^{a} Experimental data taken from refs 6 and 7. ^{b} Values calculated according to the calibration model. *ts*, compound included into training set; *na*, not available.
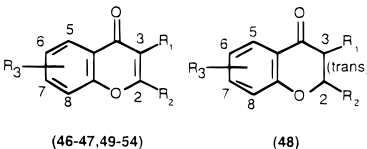
relatively rigid ring structure of flavonoids compared to other A$_3$ receptor antagonists, such as 1,4-dihydropyridines, makes them particularly amenable to CoMFA analysis.

Computational Methods

Materials and Methods. CoMFA is a three-dimensional QSAR method that operates on a set of ligands that have been superimposed to reflect their anticipated common binding orientation. CoMFA models describe the extent to which the change in magnitude of the electrostatic and steric fields as a function of compound, sampled as a function of spatial position around the compound set, accounts for the variance in measured biological activity. Molecular modeling and CoMFA studies were performed on a Silicon Graphics Power Indigo2 R8000 workstation running SYBYL 6.3.[22] Quantum calculations used throughout this study were performed using MOPAC (Ver. 6.0)[23] and Gaussian 92.[24]

Data Sets. A total of 30, 26, and 36 flavonoid derivatives were included in the training set used to generate the CoMFA models, for A$_1$, A$_{2A}$, and A$_3$ receptors, respectively. These molecules were classified into six families depending on the chemical structure of the bicyclic moiety: flavonols, **1**−**28**; flavones, **29**; flavanones, **30**−**33**; dihydroflavanols, **34**−**36**; furylchromones, **37**−**44**; and naphthoflavones, **45** (see Table 1).

Table 2. Observed and Predicted Receptor-Binding Affinity Values of the Compounds Forming A$_1$, A$_{2A}$, and A$_3$ Test Sets

(46-47,49-54)   (48)

| | | | | $pK_{i\,(\mu M)}$[a] | | | | | |
| | | | | rA$_1$ | | rA$_{2A}$ | | hA$_3$ | |
compound	R$_1$	R$_2$	R$_3$	obsd	pred[b]	obsd	pred[b]	obsd	pred[b]
46	OH	Ph	5,7-(OH)$_2$	0.06	0.11				
47 (MRS1132)	Cl	Ph	H	−0.39	−0.31				
48 (flavanone)	H	Ph	H	−1.50	−1.38				
49 (galangin)	OH	Ph	5,7-(OH)$_2$			0.01	0.11		
50	H	Ph	5-OH			−0.79	−0.73		
51	OAc	Ph	5,7-(OAc)$_2$			−1.75	−1.68		
52 (MRS1088)	Cl	Ph	6-Cl					0.13	0.19
53 (MRS1089)	OEt	2′,4′,6′-Me$_3$Ph	6-Cl					−0.72	−0.79
54 (MRS1072)	OH	CH≡CPh	6-OMe					−1.38	−1.25

[a] Experimental data taken from refs 6 and 7. [b] Values predicted by the CoMFA model.

The synthesis and binding affinity constants of all flavonoid derivatives were reported in detail previously.[6,7] Binding affinity expressed as a K_i value (inhibition constant) was obtained using the following radioligands at the respective adenosine receptors: [^{3}H]-N^6-phenylisopropyladenosine (rat A$_1$);[25] [^{3}H]CGS 21680 (rat A$_{2A}$),[26] [^{125}I]AB-MECA (human A$_3$).[27]

Molecular Superposition. The chromone moiety is believed to be a key determinant of binding interactions of flavonoid derivatives. Therefore, the ligands in this study were superimposed on the chromone nucleus by fitting a minimum-energy conformation of the compound **22** (reference structure). Conformational analysis of compound **22** was performed on the four rotatable bonds of the chromone substituents using a random search procedure in SYBYL. The energies of the resulting conformations were calculated using MOPAC (PM3 Hamiltonian, keywords: PREC, GNORM = 0.1, EF).[28] The remaining compounds were fitted by a least-squares algorithm to the reference structure so as to maximally align their substituents with the corresponding substituents of the reference structure. The fitted conformations of each compound were fully minimized using MOPAC (PM3 Hamiltonian).

Atomic Charge Calculations. Partial atomic charges are required for calculating electrostatic fields in CoMFA. Partial atomic charges for compound **22** were calculated at the semiempirical level using the MNDO,[29] AM1,[30] and PM3 Hamiltonians of MOPAC. The results of each method were compared to those obtained using the MP2/6-31G(*)//RHF/6-31G(*) ab initio level of Gaussian 92. The charges calculated using PM3 were found to agree best with the ab initio charges. Therefore, partial atomic charge for all the flavonoid derivatives were calculated using PM3 Hamiltonian. No improvements have been found using PM3 atomic charges derived from electrostatic potentials.[31]

CoMFA Field Calculations and Regression Techniques. The electrostatic and steric fields were sampled along a three-dimensional lattice encompassing all molecules in each receptor data set. The lattice consisted of 720 sample points based on a 2.0 Å lattice spacing with boundaries extending 4.0 Å beyond the largest structure in all directions. Lattice spacings of 0.75 and 1.5 Å were also used without improvements of the CoMFA results. The lattice points within the union volume of the superimposed structures were dropped. The probe used to calculate the CoMFA fields consisted of a sp^3 carbon atom with a +1 charge and a van der Waals radius of 1.52 Å. The steric and electrostatic fields were calculated separately for each molecule using a Lennard-Jones 6−12 potential and a Coulombic potential with a 1/r distance-dependent dielectric, respectively. The steric and electrostatic energies were truncated at 30 kcal/mol. The field values

corresponding to the 720 sample points for each molecule, together with binding affinity data, were stored in a SYBYL Molecular Spreadsheet to facilitate statistical analysis.

Partial least-squared (PLS) regression analysis[32] was performed on the A$_1$, A$_{2A}$, and A$_3$ antagonist datasets using a subset of CoMFA field sample points falling with a standard deviation of ≤1.0 kcal/mol. The steric and the electrostatic fields were scaled to equalize their weighting in the CoMFA models (SYBYL command "scaling CoMFA_std"). PLS was performed using cross-validation to evaluate the predictive ability of the CoMFA models.[33] The optimal number of latent variables was derived from cross-validation equation having the lowest standard error and a significance level of ≥99.5% was estimated using the stepwise F-test. Bootstrap analysis[33] of the dataset was used to evaluate the statistical confidence limits of the results. A σ value of 2.0 was adopted for both the cross-validated and non-cross-validated analysis. σ values of 1.0 or 0.5 did not significantly change the calculated r^2.

Initial PLS analyses were performed in conjunction with the cross-validation (leave-one-out method) option to obtain the optimal number of components to be used in the subsequent analyses of the dataset. The PLS analysis was repeated with the number of cross-validation groups set to zero. The optimal number of components was designated as that which yielded the highest cross-validated r^2 values in the non-cross-validated (conventional) analyses. The final PLS analysis with 10 bootstrap groups and the optimal number of components was performed on the complete dataset.

The corresponding calibration equation (resulting from the simultaneous contribution of all the observations) was derived after the optimal dimensionality of each receptor model was established, by PLS analysis and cross-validation. The calibration equation with latent variables was then converted to the original parametric space represented by probe−ligand interaction energies. A 3D-QSAR was therefore derived whose coefficients were associated with statistically significant lattice locations. CoMFA coefficient contour maps were generated by interpolation of the pairwise products between the 3D-QSAR coefficients and the standard deviations of the associated energy variables.

Test Sets. The test sets consisted of three molecules for each training set **46**−**54** (Table 2). These structures were chosen to maximize a uniform sampling of biological activity. All predicted activities for the test set molecules were calculated using the optimized CoMFA model. The results of the non-cross-validated calibration model on the test sets are summarized in Table 2.

"Predictive" r^2 Values. The "predictive" r^2_{pred} was based only on molecules not included in the training set and is defined as explained by Marshall and co-workers.[34]

Table 3. Statistic of the Calibration CoMFA Models

	A_1	A_{2A}	A_3
number of compounds	30	26	36
principal components[a]	6	4	6
r^2_{cv}[b]	0.605	0.595	0.583
r^2	0.961	0.963	0.957
F_{test}[c]	87.541	125.192	119.53
p value	<0.001	<0.001	<0.001
r^2_{bs}[d]	0.985	0.978	0.974
Steric contribution	0.492	0.486	0.460
Electrostatic contribution	0.508	0.514	0.540
SEP[e]	0.086	0.112	0.108
std dev[f]	0.011	0.015	0.012

[a] Minimum $\sigma = 2.0$. [b] Standard error of prediction (cross-validated) = $(PRESS/(n - c - l))^{1/2}$, n = number of rows, c = number of components. [c] Ratio of r^2 explained to unexplained = $r^2/(l - r^2)$. [d] r^2_{bs} = r^2 after bootstrapping. [e] Cross-validated r^2 after leave-one-out procedure: r^2_{cv} = (SD − PRESS)/SD, SD = Y_{actual} − $Y_{mean})^2$. PRESS = $\Sigma(Y_{predicted} - Y_{actual})$. For further explaination of these mathematical formulas see ref 33. [f] Std dev column belongs with the bootstrapping r^2.

Results

CoMFA of A_1 Receptor Binding Affinity. PLS was used in conjunction with cross-validation to obtain the optimal number of components to be used in the subsequent analyses. PLS analysis based on least-squares fit gave a correlation with a cross-validated r^2_{cv} of 0.605, with the maximum number of components set equal to 6 (maximum number of components set equal to 4, 5, 7, or 8 gave unreliable cross-validated $r^2_{cv} \leq 0.40$) and the cross-validation groups set equal to the number of observations (rows) in the data table. The non-cross-validated PLS analysis was repeated with the optimum number of components, as determined by the cross-validated analysis, to give an r^2_{cv} of 0.961. To obtain statistical confidence limits, the non-cross-validated analysis was repeated with 10 bootstrap groups, which yielded an r^2 of 0.985 (optimum number of components was 6), SEP = 0.086, std dev = 0.011, steric contribution = 0.492, and electrostatic contributions = 0.508. These parameters are explained in Table 3.

The CoMFA-derived QSAR of the A_1 ligands exhibited a good cross-validated correlation, indicating that it was highly predictive. Cross-validation provides information concerning the predictive ability of the QSAR dataset by minimizing the occurrence of chance correlations in the QSAR model. The high bootstrapped r^2 value and small standard deviation suggest a high degree of confidence in the analysis. The calculated binding affinities obtained from the analysis were plotted versus the actual values in Figure 1.

Compounds **46−48** (test set) were used to evaluate the predictive power of this CoMFA model. As in the calibration step, a good predictive ability with an r^2_{pred} = 0.858 for the compounds in the test set was obtained. Table 2 shows that the affinities of all the examined compounds are predicted within 0.12 log unit across a range of 1.56 log units.

The coefficients corresponding to each sampled field point in the resulting correlation equation were graphically contoured. Contours corresponding to the steric (green and yellow) and electrostatic (blue and red) fields are plotted together with compound **2** in Figure 2. The polyhedra describe the regions of space where the steric and the electrostatic fields are predicted by the CoMFA model to have the greatest effect on binding affinity.
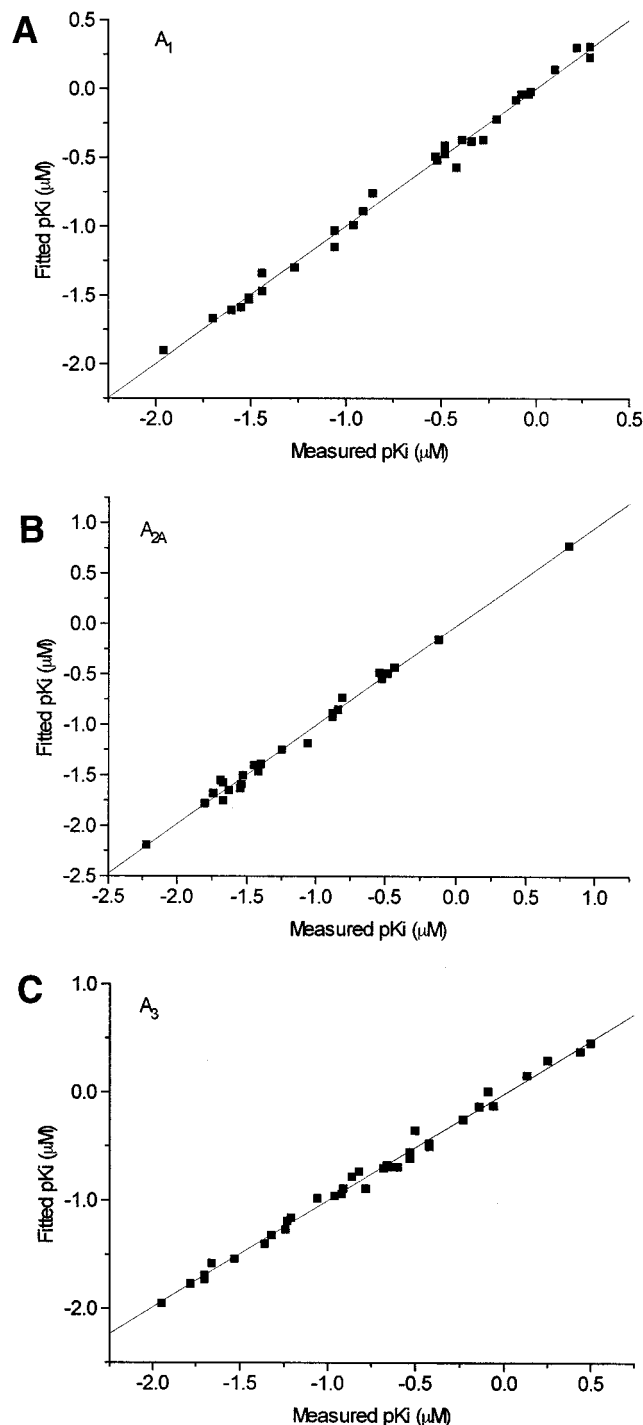

Figure 1. Fitted vs measured pK_i values for the CoMFA analysis of the A_1, A_{2A}, and A_3 training sets (A, B, and C, respectively). A_1: the model was derived using six principal components yielding a cross-validated r^2 = 0.605. A_{2A}: the model was derived using four principal components yielding a cross-validated r^2 = 0.595. A_3: the model was derived using six principal components yielding a cross-validated r^2 = 0.583.

The yellow and the blue polyhedra correspond to regions of the field that are predicted to decrease the A_1 receptor affinity, whereas the green and the red regions are predicted to increase binding affinity. The region of space around the para position of the phenyl ring is contained within a yellow (steric detracting) polyhedron, suggesting that bulky substituents are not tolerated by the receptor at the C-2 position of the chromone moiety.
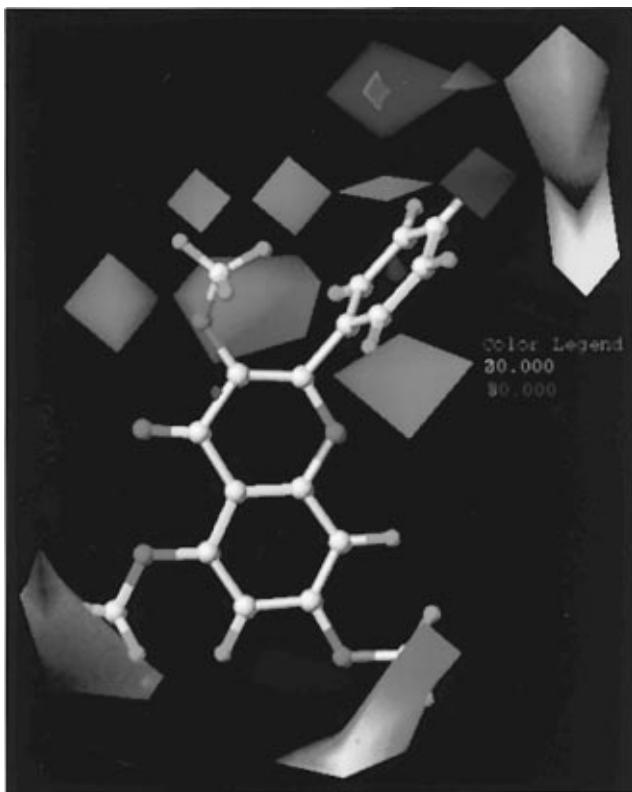
Figure 2. CoMFA steric and electrostatic STDEV*COEFF contour plots from the analysis based on the A_1 receptor 3D-QSAR without cross-validation. Compound **2** shown inside the field. Favoring activity: green, bulky group (contribution level 80%); yellow, less bulky; blue, positive charge (contribution level 70%); red, negative charge.

Figure 3. CoMFA steric and electrostatic STDEV*COEFF contour plots from the analysis based on the A_{2A} receptor 3D-QSAR without cross-validation. Compound **45** shown inside the field. Favoring activity: green, bulky group (contribution level 80%); yellow, less bulky; blue, positive charge (contribution level 70%); red, negative charge.

Both styryl and phenylpropargyl derivatives (see compounds **35**−**36**, Table 1) are in fact among the less active compounds. The C-5 and C-7 positions of the chromone structure are surrounded by green polyhedra, suggesting that the presence of alkoxy substituents increases A_1 receptor affinity (see compounds **2**−**3**, Table 1). The regions of space around the ortho positions of the phenyl ring are contained within a large red contour, suggesting that substituents that enhance the electrostatic fields in that region improve the A_1 receptor binding affinity. An *o*-hydroxy substituent (compound **31**, Table 1) could be expected to improve affinity electrostatically, whereas bulky alkoxy substituents (**9**−**13**) would also detract sterically. The blue polyhedron around the para position of the phenyl ring suggests that substituents with higher electron density at this position may reduce the binding affinity. The red polyhedron around the C-3 chromone position is in agreement with the know enhancement in A_1 binding affinity produced by alkoxy substituents at this position (**22, 24**).

CoMFA of A_{2A} Receptor Binding Affinity. The chosen alignment yielded good cross-validated ($r^2_{cv} = 0.595$) and conventional results ($r^2 = 0.963$, *F*-test value = 125.192), with the optimal number of components found equal to 4. Steric and electrostatic fields contribute to the QSAR equation by 48.6% and 51.4%, respectively. A high bootstrapped (10 sampling) r^2_{bs} value of 0.978 (SEP = 0.112, std dev = 0.015) was found. The calculated binding affinities obtained from the analysis are plotted versus the actual values in Figure 1.
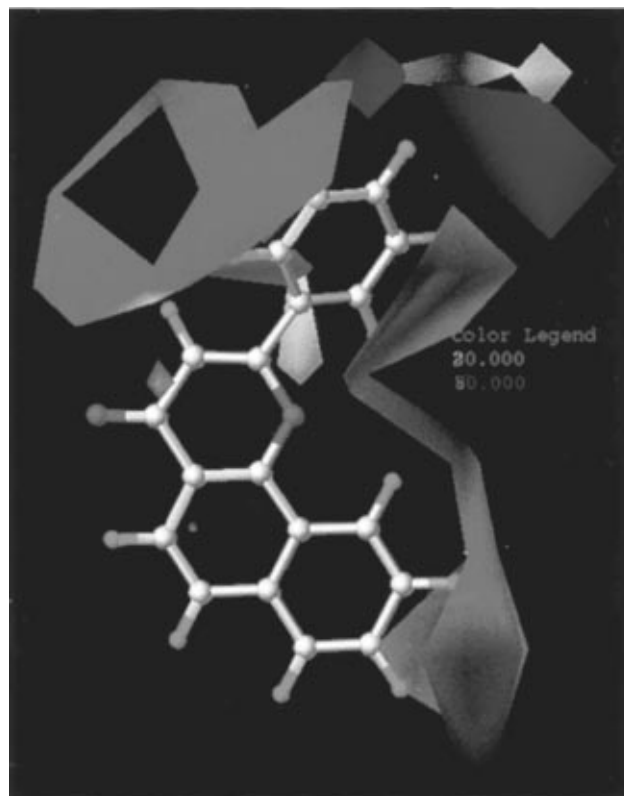
Compounds **49**−**51** (test set) were used to evaluate the predictive power of this CoMFA model. A good predictive ability with an $r^2_{pred} = 0.835$ for the compounds in the test set was obtained in this calibration step. Table 2 shows that the affinities of all compounds examined are predicted within 0.10 log unit across a range of 1.76 log units.

Contours corresponding to the steric (green and yellow) and electrostatic (blue and red) fields are plotted together with compound **45** in Figure 3. A green contour around the C-3 position of the chromone moiety suggests that bulky substituents in this position (see compounds **1**, **3**, and **5**, Table 1) enhance affinity. Another important area of bulk tolerance is found around the C-7 and C-8 positions of the chromone moiety. In fact, α-naphthoflavone (**45**) presents a good affinity and a very high selectivity. As for the A_1 model, bulky substituents in the C-2 position of chromone moiety decrease the A_{2A} receptor affinity (see compounds **35**−**36**). The blue polyhedron around the para position of the phenyl ring suggests that substituents with higher electron density exert a negative effect on the affinity, in agreement with the experimental data that alkoxy substituents in this position decrease the A_{2A} receptor affinity (**19, 24**).

CoMFA of A_3 Receptor Binding Affinity. The chosen alignment yielded acceptable cross-validated ($r^2_{cv} = 0.583$) and conventional results ($r^2 = 0.957$, *F*-test value = 119.53), with the optimal number of components found to be equal to 6. In this model, steric and electrostatic fields contribute to the QSAR equation by
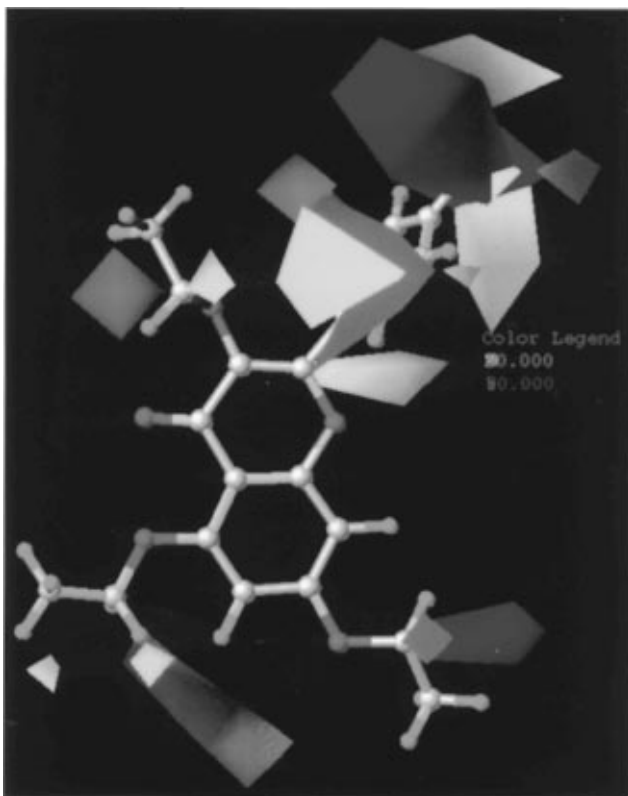
Figure 4. CoMFA steric and electrostatic STDEV*COEFF contour plots from the analysis based on the A₃ receptor 3D-QSAR without cross-validation. Compound **3** shown inside the field. Favoring activity: green, bulky group (contribution level 80%); yellow, less bulky; blue, positive charge (contribution level 70%); red, negative charge.

46.0% and 54.0%, respectively. A high bootstrapped (10 sampling) r^2bs value of 0.974 (SEP = 0.108, std dev = 0.012) was found. Compounds **52−54** (test set) were used to evaluate the predictive power of this CoMFA model. The predicted binding affinities obtained from the analysis are plotted versus the actual values in Figure 1. A good predictive ability with an r^2_{pred} = 0.817 for the compounds in the test set was obtained as for the calibration steps. Table 2 shows that the affinities of all the examined compounds are predicted within 0.13 log unit across a range of 1.51 log units.

Contours corresponding to the steric (green and yellow) and electrostatic (blue and red) fields are plotted together with compound **3** in Figure 4. As for A₁ and A₂A receptor CoMFA models, the major variability of the steric contour maps occurs around the phenyl ring on the C-2 position of the chromone moiety. Again, a yellow area surrounds the para position of the phenyl ring, suggesting that bulky substituents are not tolerated at the C-2 position of the chromone moiety. Bulky groups are also predicted to be tolerated around the C-6 position of the chromone moiety for A₃ receptor binding. In fact, the presence of a chloro substituent in this position is tolerated (**13**). The area of bulky tolerance surrounding the ortho position of the phenyl ring suggests that bulky substituents at this position may increase A₃ affinity. A 2′-*i*-Pr derivative (**13**), in fact, displays good affinity. Bulky substituents at the C-2 position of the chromone moiety decrease the affinity also for the A₃ receptor (see compounds **35−36**). The blue polyhedron in the para position of the phenyl ring

indicates that substituents with higher electron density exert a negative effect on the affinity, in agreement with the experimental data that alkoxy substituents in this position decrease the A₃ receptor affinity (**10, 18**).

Discussion

A set of 3D-QSAR models has been developed using the CoMFA methodology for flavonoid derivative adenosine receptor antagonists. This is the first attempt to describe quantitatively the hypothetical receptor binding site of multiple subtypes of adenosine receptors. Comparison of the three CoMFA models helps in understanding adenosine receptor selectivity. The analysis of these results leads to the following considerations:

(a) All three CoMFA models have similar average steric and electrostatic contributions (see Table 3), implying that A₁, A₂A, and A₃ have the same relative contribution of steric and electrostatic factors inside the binding cavity. However, the specific distribution of steric and electrostatic interactions for each receptor is different, as shown in Figures 2−4.

(b) Similarities were seen in the topology of steric and electrostatic regions with the A₁ and A₃ receptors, but not the A₂A receptor (Figures 2−4). This is in accord with the structure−activity relationship data in which A₁−A₃ similarity has been demonstrated.[17]

(c) C-2 chromone phenyl ring substituents are considered important for the binding affinity for all adenosine receptors. This phenyl ring may interact in a similar region of space inside the receptor binding-site.

(d) An interesting consideration about A₁/A₃ selectivity can be deduced from CoMFA contour map analysis. An important green region (favorable steric bulk interaction) is located around the 2′-position of the phenyl ring, in the A₃ model. This is in accord with the experimental data for compounds **8**, **12**, and **13**, which are the most selective flavonoid compounds for human A₃ receptors.

(e) The presence of a C-6 substituent in the chromone moiety is well tolerated, and increases the A₁/A₃ selectivity (see compound **13**).

Further synthesis and biological evaluation of new flavonoid derivatives aimed at increasing both the affinity and the selectivity for the adenosine receptors are in progress.

Conclusion

In conclusion, the CoMFA method has been successfully applied to a set of recently described flavonoid derivatives with affinity for A₁, A₂A, and A₃ receptors. The resulting 3D-QSAR models show good correlations between steric and electrostatic field and binding affinities. The CoMFA coefficient contour plots provide a self-consistent picture of the main chemical features responsible for the pK_i variations, and the CoMFA QSAR equations result in predictions which agree with the experimental values. Comparison of our CoMFA models can be used to suggest improvement of adenosine receptor subtype selectivity. This information may be useful for designing new compounds with higher selectivity for A₃ vs A₁ and A₂A receptors.

Abbreviations

3D-QSAR, three-dimensional quantitative structure activity relationship; [¹²⁵I]AB-MECA, N^6-(4-amino-3-

iodobenzyl)adenosine 5′-*N*-methyluronamide; Cl-IB-MECA, N^6-(3-iodobenzyl)-2-chloroadenosine 5′-*N*-methyluronamide; CoMFA, comparative molecular field analysis; PLS, partial least-squares; QSAR, quantitative structure−activity relationship; r^2_{bs}, correlation coefficient from boostrap analysis; r^2_{cv}, correlation coefficient from cross-validation equation; rms, root-mean-square.

References

(1) Jacobson, K. A.; Suzuki, F. Recent Developments in Selective Agonists and Antagonists Acting at Purine and Pyrimidine Receptors. *Drug Dev. Res.* **1997**, *39*, 289−300.

(2) Müller, C. A₁ Adenosine Receptor Antagonists. *Exp. Opin. Ther. Patents* **1997**, *7*, 419−440.

(3) von Lubitz, D. K. J. E.; Lin, R. C. S.; Popik, P.; Carter, M. F.; Jacobson, K. A. Adenosine A₃ Receptor Stimulation and Cerebral Ischemia. *Eur. J. Pharmacol.* **1994**, *263*, 59−67.

(4) Strickler, J.; Jacobson, K. A.; Liang, B. T. Direct Preconditioning of Cultured Chick Ventricular Myocytes: Novel Functions of Cardiac Adenosine A₂ₐ and A₃ Receptors. *J. Clin. Invest.* **1996**, *74*, 1773−1779.

(5) Sajjadi, F. G.; Takabayashi, K.; Foster, A. C.; Domingo, R. C.; Firestein, G. S. Inhibition of TNF-alpha Expression by Adenosine−Role of A₃ Adenosine Receptors. *J. Immunol.* **1996**, *156*, 3435−3442.

(6) Ji, X.-d.; Melman, N.; Jacobson, K. A. Interactions of Flavonoids and Other Phytochemicals with Adenosine Receptors. *J. Med. Chem.* **1996**, *39*, 781−788.

(7) Karton, Y.; Jiang, J. L.; Ji, X.-d.; Melman, N.; Olah, M. E.; Stiles, G. L.; Jacobson, K. A. Synthesis and Biological-Activities of Flavonoid Derivatives as as Adenosine Receptor Antagonists. *J. Med. Chem.* **1996**, *39*, 2293−2301.

(8) van Rhee, A. M.; Jiang, J. L.; Melman, N.; Olah, M. E.; Stiles, G. L.; Jacobson, K. A. Interaction of 1,4-Dihydropyridine and Pyridine Derivatives with Adenosine Receptors − Selectivity for A₃ Receptors. *J. Med. Chem.* **1996**, *39*, 2980−2989.

(9) Jiang, J.-l.; van Rhee, A. M.; Chang, L.; Patchornik, A.; Evans, P.; Melman, N.; Jacobson, K. A. Structure Activity Relationships of 4-Phenylethynyl-6-phenyl-1,4-dihydropyridines as Highly Selective A₃ Adenosine Receptor Antagonists *J. Med. Chem.* **1997**, *40*, 2596−2608.

(10) Kim, Y.-C.; Ji, X.-d.; Jacobson, K. A. Derivatives of the Triazoloquinazoline Adenosine Antagonist (CGS15943) are Selective for the Human A₃ Receptor Subtype. *J. Med. Chem.* **1996**, *39*, 4142−4148.

(11) Jacobson, M. A.; Chakravarty, P. K.; Johnson, R. G.; Norton, R. Novel Selective Nonxanthine A₃ Adenosine Receptor Antagonists. *Drug Dev. Res.* **1996**, *37*, 131.

(12) Beaven, M. A.; Ramkumar, V.; Ali, H. Adenosine A₃ Receptors in Mast Cells. *Trends Pharmacol. Sci.* **1994**, *15*, 13−14.

(13) Jacobson, K. A.; Kim, H. O.; Siddiqi, S. M.; Olah, M. E.; Stiles, G.; von Lubitz, D. K. J. E. A₃ Adenosine Receptors: Design of Selective Ligands and Therapeutic Prospects. *Drugs Future* **1995**, *20*, 689−699.

(14) Jacobson, K. A.; Park, K. S.; Jiang, J.-l.; Kim, Y.-C.; Olah, M. E.; Stiles, G. L.; Ji, X.-d. Pharmacological Characterization of Novel A₃ Adenosine Receptor-Selective Antagonists. *Neuropharmacology* **1997**, *36*, 1157−1165.

(15) Shin, Y.; Daly, J. W.; Jacobson, K. A. Activation of Phosphoinositide Breakdown in a Rat RBL-2H3 Mast Cell Line by Adenosine Analogues: Lack of Correlation with Affinity for A₃-Adenosine Receptor. *Drug Dev. Res.* **1996**, *39*, 36−46.

(16) Linden, J.; Taylor, H. E.; Robeva, A. S.; Tucker, A. L.; Stehle, J. H.; Rivkees, S. A.; Fink, J. S.; Reppert, S. M. Molecular Cloning and Functional Expression of a Sheep A₃ Adenosine Receptor with Widespread Tissue Distribution. *Mol. Pharmacol.* **1993**, *44*, 524−532.

(17) Salvatore, C. A.; Jacobson, M. A.; Taylor, H. E.; Linden, J.; Johnson, R. G. Molecular Cloning and Characterization of the Human A₃ Adenosine Receptor. *Proc. Natl. Acad. Sci. U.S.A.* **1993**, *90*, 10365−10369.

(18) Middleton, E., Jr. Some Biological Properties of Plant Flavonoids. *Ann. Allergy* **1988**, *61* 53−57.

(19) Limasset, B.; le Doucen, C.; Dore, J. C.; Ojasoo, T.; Damon, M.; Crastes de Paulet, A. Effects of Flavonoids on the Release of Reactive Oxygen Species by Stimulated Human Neutrophils. Multivariate Analysis of Structure−Activity Relationships (SAR). *Biochem. Pharmacol.* **1993** *46*: 1257−1271.

(20) Raghavan, K.; Buolamwini, J. K.; Kohn, K. W.; Weinstein, J. N. Three-Dimensional Quantitative Structure−activity Relationship (QSAR) of HIV Integrase Inhibitors: A Comparative Molecular Field Analysis (CoMFA) Study. *J. Med. Chem.* **1995**, *38*, 890−897.

(21) Dai, R.; Jacobson, K. A.; Robinson, R. C.; Friedman, F. K. Differential Effects of Flavonoids on Testosterone-Metabolizing Cytochrome P450s. *Life Sci. Pharmacology Lett.* **1997**, *61*, PL75−PL80.

(22) The program SYBYL 6.3 is available from TRIPOS Associates, St. Louis, MO, 1993.

(23) MOPAC 6.0 available from Quantum Chemistry Program Excange.

(24) Frisch, M. J.; Trucks, G. W.; Head-Gordon, M.; Gill, P. M. W.; Wong, M. W.; Foresman, J. B.; Johnson, B. G.; Schlegel, H. B.; Robb, M. A.; Replogle, E. S.; Gomperts, R.; Andres, J. L.; Raghavachari, K.; Binkley, J. S.; Gonzalez, C.; Martin, R. L.; Fox, D. J.; Defrees, D. J.; Baker, J.; Stewart, J. J. P.; Pople, J. A. *Gaussian 92*, Gaussian, Inc.: Pittsburgh, PA, 1992.

(25) Schwabe, U.; Trost, T. Characterization of adenosine receptors in rat brain by (−)[³H]N⁶-phenylisopropyladenosine. *Naunyn-Schmiedeberg's Arch. Pharmacol.* **1980**, *313*, 179−187.

(26) Jarvis, M. F.; Schutz, R.; Hutchison, A. J.; Do, E.; Sills, M. A.; Williams, M. [³H]CGS 21680, an A₂ Selective Adenosine Receptor Agonist Directly Labels A₂ Receptors in Rat Brain Tissue. *J. Pharmacol. Exp. Ther.* **1989**, *251*, 888−893.

(27) Olah, M. E.; Gallo-Rodriguez, C.; Jacobson, K. A.; Stiles, G. L. [¹²⁵I]AB-MECA, a High Affinity Radioligand for the Rat A₃ Adenosine Receptor. *Mol. Pharmacol.* **1994**, *45*, 978−982.

(28) Stewart, J. J. P. Optimization of Paramiters for Semiempirical Methods I. Methods. *J. Comput. Chem.* **1989**, *10*, 209−217.

(29) Dewar, M. J. S.; Thiel, W. Ground States of Molecules. 38. The MNDO method. Approximations and Parameters. *J. Am. Chem. Soc.* **1977**, *99*, 4899−4905.

(30) Dewar, M. J. S. E.; Zoebisch, G.; Healy, E. F. AM1: A New General Purpose Quantum Mechanical Molecular Model. *J. Am. Chem. Soc.* **1985**, *107*, 3902−3909.

(31) Chirlian, L. E.; Francl, M. M. Atomic Charges Derived from Electrostatic Potentials: A Detailed Study. *J. Comput. Chem.* **1987**, *8*, 894−905.

(32) Wold, S.; Ruhe, A.; Wold, H.; Dunn, W. J. The Covariance Problem in Linear Regression. The Partial Least Squares (PLS) Approach to Generalized Inverses. *SIAM J. Sci. Stat. Comput.* **1994**, *5* (3), 735−743.

(33) Cramer, R. D.; Bunce, J. D.; Patterson, D. E.; Frank, I. E. Crossvalidation, Bootstrapping, and Partial Least Squares Compared with Multiple Regression in Conventional QSAR Studies. *Quantum Struct.-Act. Relat.* **1988**, *7*, 18−25.

(34) Waller, C. L.; Oprea, T. I.; Giolitti, A.; Marshall, G. R. Three-Dimensional QSAR of Human Immunodeficiency Virus (I) Protease Inhibitors. 1. A CoMFA Study Employing Experimentally-Determined Alignment Rules. *J. Med. Chem.* **1993**, *36*, 4152−4160.